DOI: 10.21062/mft.2024.058  http://www.journalmt.com

# Effect of Filler Content and Treatment on Mechanical Properties of Polyamide Composites Reinforced with Short Carbon Fibres Grafted with Nano-$SiO_2$

Dana Bakošová (0000-0003-2936-8637), Alžbeta Bakošová (0000-0003-3440-0689), Petra Dubcová (0000-0003-3450-3290), Daniela Koštialiková (0000-0003-4981-7698), Andrej Dubec (0009-0001-6145-6357), Mariana Janeková (0000-0002-9380-2760)
Faculty of Industrial Technologies in Púchov, Alexander Dubček University of Trenčín. I. Krasku 491/30, 020 01 Púchov. Slovakia. E-mail: dana.bakosova@tnuni.sk, alzbeta.bakosova@tnuni.sk, petra.dubcova@tnuni.sk, daniela.kostialikova@tnuni.sk, andrej.dubec@tnuni.sk, mariana.janekova@tnuni.sk

**The polyamide PA6 composites reinforced with carbon fibres (CF) are widely studied due to their properties and their high strength to weight ratio. Good adhesion between a filler and a matrix is essential for enhancing properties of a resulting composite. This study investigates the effect of the short CF content and the used CF treatment on mechanical properties of the PA6-CF composites. The composites were subjected to tensile, flexural, compression, hardness and Charpy tests as well as dynamical mechanical analysis. An atomic force microscopy was employed to investigate topography of the CF and the composites. Initially, the properties of the composites were improved through the oxidation of the CF in $HNO_3$. Subsequently, to further enhance these properties, the oxidized CF were grafted with nano-$SiO_2$. The CF content in the tested composites varied from 10 wt% to 60 wt%. The most significant improvement of the tested properties was observed at the CF content of 40 wt%.**

**Keywords:** Polyamide composites, Carbon Fibres, Nano-silica, Fibre surface treatment, Mechanical properties

## 1 Introduction

Polymers reinforced with carbon fibres (CF) stand out with their high strength to weight ratio, which paired with their excellent thermal, electrical, structural and tribological properties designates them as alternative to conventional metal structural materials. Due to their exceptional properties, carbon fibre reinforced composites are widely used in various applications such as automotive, aerospace industry, sport equipment and wind energy. For high performance applications thermoplastic matrices are used including polyamide (PA), polyethylene terephthalate (PET), polycarbonate (PC), polyetheretherketone (PEEK) among others [1]-[4].

The synthetized CF are inert, non-polar material with smooth surface, thus they have poor affinity to some polymers, which are generally polar. Therefore, to utilize their full reinforcement potential their surface is treated to ensure good interfacial adhesion between the CF and the polymer matrix [4]. The adhesion can be improved by physico-chemical processes, by which reactive functional groups are created on the CF surface, mechanical processes, that increase roughness of the CF surface or their combination [5]. Various approaches [6] to enhance adhesion to polymer matrix include oxidation [7]-[9], chemical grafting [10], chemical deposition [11], [12], sizing agent coating [13], [14], coating with nanofillers [15], plasma treatment [16], microwave irradiation [17].

Polyamide 6 (PA6) is widely used matrix of CF reinforced polymer composites, due to its good mechanical properties, chemical resistance and versatility. It has good wear resistance and a low coefficient of friction, making it suitable for applications where friction and abrasion occur. The PA6 has a relatively high melting point (around 220 °C), which allows it to withstand elevated temperatures. It can be easily processed using a variety of manufacturing methods, including injection moulding, extrusion and blow moulding, enabling the production of complex shapes and parts [18], [19].

Thanks to their material properties, the PA6-CF composites are broadly researched. The properties of final composites are affected by several factors. Besides used types of the matrix and fibres, the properties also depend on manufacturing processes, orientation and concentration of the fibres [20], [21], and their adhesion to the matrix. Effects of CF length and content, on the mechanical, thermal and morphological properties of the PA6-CF composites prepared by melt mixing method were investigated in the work [21]. The increase in the tensile strength, modulus and hardness values and the decrease in elongation at break with the increasing CF content were reported. The glass transition temperature and melting temperature were not changed significantly. Heat of fusion and the relative degree of crystallinity values of composites decreased with the ascending CF content.

The storage and loss moduli values of composites increased with the increasing CF content. Similar results were observed also in the study [22]. In the study [23], mechanical properties of CF composites with various CF content up to 30 wt% and different polymer matrices (polypropylene, polyethylene, polyamide 6 and polyamide 12) were compared. The results of tensile and tree-point flexural tests indicate significant increase in the mechanical properties of the CF composites. However, it is observed that the percentage increase in mechanical properties reduces as the CF content rise, as improvement is more pronounced when comparing composites with the CF content of 0 wt% and 10 wt% than when comparing those with 20 wt% to 30 wt% CF content. Besides the CF content, evaluated mechanical properties were significantly affected by matrix type of the composites. The best results were observed in PA6 composites due to better mechanical properties of PA6 compared to other matrices.

Nanoparticles are widely used to improve adhesion between the CF and polymer matrix, including carbon nanotubes [24], nanosilica ($SiO_2$) [6], [25], [26], graphene oxide [27] and titanium dioxide [28]. In the study [25], the short CF reinforced PA6 composite with polydopamine/nanosilica (PDA-$SiO_2$) interfacial layer on the CF surface was studied and a 28.09% increase in strength was observed compared to the untreated CF. In the study [10] the interfacial adhesion of PA6 composites reinforced with CF was investigated. The CF were oxidized, modified with 3-aminopropyltriethoxysilane and then grafted with $SiO_2$ nanoparticles. The $SiO_2$ nanoparticles uniformly distributed on the CF surface improved interfacial adhesion between CF and PA6 and improvement in the strength compared to composites with untreated CF was observed. In the study [26], polyurethane with nano-$SiO_2$ was used to size continuous CF filaments to enhance their compatibility with PA6 matrix, resulting in improved mechanical properties and 20.75% increase in tensile strength compared to the composites with untreated CF.

This study focuses on the enhancement of the PA6 composites reinforced with chopped short CF. The effect of different modification methods applied to the CF and variation of the CF content on the mechanical properties of the resulting PA6-CF composites is investigated. Three groups of PA6-CF composites were tested: the first group comprised composites produced with the unmodified CF, the second group was produced with the CF oxidized in $HNO_3$ and in the last group, the CF were oxidized in $HNO_3$ and subsequently grafted with nano-$SiO_2$. Each group encompassed composites with a different CF content, spanning from 10 to 60 wt%. The PA6 specimens without CF reinforcement were also examined for comparative analysis.

## 2 Materials

The polyamide PA6 matrix was reinforced with the short, chopped CF, which were made by precision cutting from a continuous carbon fibre. Selected material properties of the used CF are listed in the Tab. 1. The mechanical properties of the CF composite materials depend on the adhesion between the fibres and a polymer matrix. Therefore, the CF surface treatments are utilized to improve the adhesion. In this study, three types of the short CF were used:

- The CF without treatment – in order to remove all impurities from the surface, the CF were cleaned in acetone for 20 minutes.
- The CF oxidized in $HNO_3$ – the CF were oxidized and mixed in $HNO_3$ at a temperature of 80 °C for 5 hours, then washed with deionized water and dried in an oven. Treatment of the CF with nitric acid can increase their surface energy and form functional groups, which can lead to better adhesion between the CF and the polyamide matrix. Additionally, it can facilitate their better dispersion in the polyamide matrix, resulting in a more homogeneous material with better mechanical properties.
- The CF grafted with nano-$SiO_2$ – the CF oxidized in $HNO_3$ were mixed in a toluene solution containing 4% of nano-$SiO_2$ powder at a temperature of 90 °C for 6 hours, then washed with ethanol and dried. Grafting with the $SiO_2$ nanoparticles can improve the adhesion between the CF and the polyamide matrix, leading to better load transfer and higher mechanical strength of the composite. Moreover, they can aid in dispersing the CF and preventing the formation of agglomerates, allowing better homogeneity of the composite. The presence of $SiO_2$ can increase the thermal stability of the composite, thermal conductivity and resistance to thermal shocks [25].

***Tab. 1*** *Material properties of the used CF*

| | |
|---|---|
| **Density** | 1.80 g/cm$^3$ |
| **Fiber length** | 3 mm |
| **Fiber diameter** | 7 μm |
| **Tensile strength** | 4 GPa |
| **Tensile modulus** | 240 GPa |
| **Combability with** | PEEK, PEI, PA, polyamides |

Three variants of composite materials PA6-CF were prepared. The first variant contained the CF without surface treatment. The second variant of the samples was prepared with CF oxidized in $HNO_3$ and the last one contained the CF grafted with nano-$SiO_2$. For each variant, samples were prepared with a different CF content in the range of 10 – 60 wt% (specifically 10, 15, 20, 30, 40, 50 and 60 wt%). The composite samples were labelled based on the CF concentration: PA6-CF10, PA6-CF15, PA6-CF20, PA6-CF30, PA6-CF40, PA6-CF50, and PA6-CF60. In addition to the PA6-CF composites, PA6 matrix material samples were also tested as reference.

Pellets (Fig. 1) for the production of the PA6-CF composites were prepared by melt mixing using a co-rotating twin-screw extruder (the speed of the first screw was 50 rpm, the speed of the second screw was 120 rpm). The PA6 was fed into a hopper and the carbon fibres were simultaneously added. By rotating the second screw, they were dispersed in the PA6 matrix at a temperature in the range of 270 – 290 °C for 5 minutes. Then, the extruded material was cooled in a water bath and divided into pellets measuring 4 – 5mm in length. These pellets were dried in an oven for 24 h at 80 °C to remove residual water prior to injection moulding.


***Fig. 1*** *Examples of PA6 pellets, short chopped CF and PA6-CF pellets*

Specimen were prepared according to relevant standards using injection moulding machine. The injection parameters are listed in the Tab. 2. The moulding scheme with indicated temperature zones is in the Fig. 2.

***Tab. 2*** *The injection parameters (temperature zones are numbered in the Fig. 2)*

| Parameter | Value |
|---|---|
| Drying temperature and time (1) | 80 °C, 24 hours |
| Feed section temperature (2) | 80 °C |
| Barrel temperature (3) | 240 – 300 °C |
| Nozzle temperature (4) | 270 – 300 °C |
| Melt temperature (5) | 270 – 300 °C |
| Mold temperature (6) | 100 – 120 °C |
| Holding pressure | 700 – 800 bar |
| Back pressure | 120 – 150 bar |
| Injection speed | 170 – 180 $cm^3/s$ |
| Screw speed | 100 rpm |

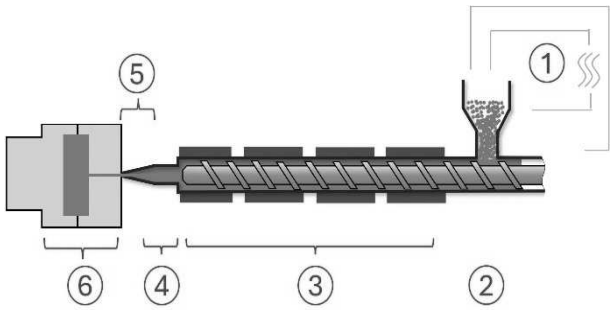


***Fig. 2*** *Injection moulding scheme*

## 3 Experimental methods

The mechanical properties of each PA6-CF composite were investigated utilizing following measurements:

- Tensile tests (ISO 527) were performed at 20 °C and loading speed 50 mm/min. Type 5 specimens with a gauge length of 50 ±0.1 mm and a thickness of 3 ±0.1 mm were used. Tensile strength, tensile modulus and elongation at break were determined. An extensometer was also used to obtain more accurate elongation data.

- Three-point flexural tests (ISO 178) were performed using method A at temperature of 20°C and loading speed 2 mm/min. The specimens measured 80 ±0.1 mm in length and 10 ±0.1 mm in width, with a thickness of 4 ±0.1 mm. The distance between the supports was 64 ±1 mm.
- Compressive tests (ISO 604) were carried out at 20 °C, using the specimens with the following dimensions: length 10 ±0.1 mm, width 10±0.1 mm and thickness 4 ±0.1 mm.
- The hardness tests were conducted using the Shore D method (ISO 868) at 20 °C.
- The Charpy tests (ISO 179) were performed at temperatures of 20°C and -30°C, using test samples with a type A notch. The samples were 80 ±0.1 mm long, 10 ±0.1 mm wide and 4 ±0,1 mm thick. Charpy notched impact strength was evaluated.
- The temperature and frequency dynamic mechanical analysis (DMA) sweeps were carried out, using the 20 ±0.1 mm long, 10 ±0.1 mm wide and 2 ±0.1 mm thick specimens. They were subjected to tensile stress in the temperature range of -80 to 200 °C using a heating rate of 15 °C/min at a frequency of 1 Hz. A cryogenic nitrogen container was used to apply low temperatures. The frequency sweep was performed in the range of 0.01 Hz to 50 Hz at a temperature of 20 °C.

The tests were performed on 10 specimens of each material. After production, the specimens were stored for 7 days at laboratory temperature of 20 °C in order to stabilize the properties. All specimens were placed in a dehumidifier for 24 hours at 80 °C before the test, as humidity can affect the physical properties of polyamides. The MATLAB was used to process and evaluate the experimental data.

Furthermore, the atomic force microscopy (AFM) was employed to investigate topography of the PA6-CF composites and the surface modification of the CF using the AFM NT-206 microscope. Quantitative measurements of sample topography by the AFM enable important metrological assessments such as roughness profile, roughness parameters, detection of surface roughness, as well as more advanced measurements such as skewness and kurtosis of the assessed profile [29], [30]. The used microscope allows evaluation of maximum profile peak height, nominal length of the profile, actual length of the profile, arithmetic mean deviation Ra, root mean square deviation of the assessed profile Rq, skewness and kurtosis. To analyse the roughness of the tested materials parameters Ra and Rq were determined, as they are commonly used [10], [31]. The roughness was evaluated using the AFM NT-206 software, by processing the statistical value of z-heights of the imaged surface area

## 4 Results and discussion

### 4.1 Topography

Firstly, the CF surface of untreated as well as the surface of the CF subjected to treatments was examined by the AFM and roughness parameters Ra and Rq were determined. The corresponding topography is shown in the Fig. 3 and the values of Ra and Rq are listed in the Tab. 3. The surface of the unmodified CF was the smoothest. Oxidation of the CF in $HNO_3$ led to an increase in the surface roughness and the CF grafted with nano-$SiO_2$ had a surface coating of the highest roughness. Through the evaluation of the treated CF surface, it is evident that oxidation in $HNO_3$ followed by grafting of nano-$SiO_2$ effectively enhances surface roughness. This enhancement facilitates improved adhesion between the CF and the polymer matrix.

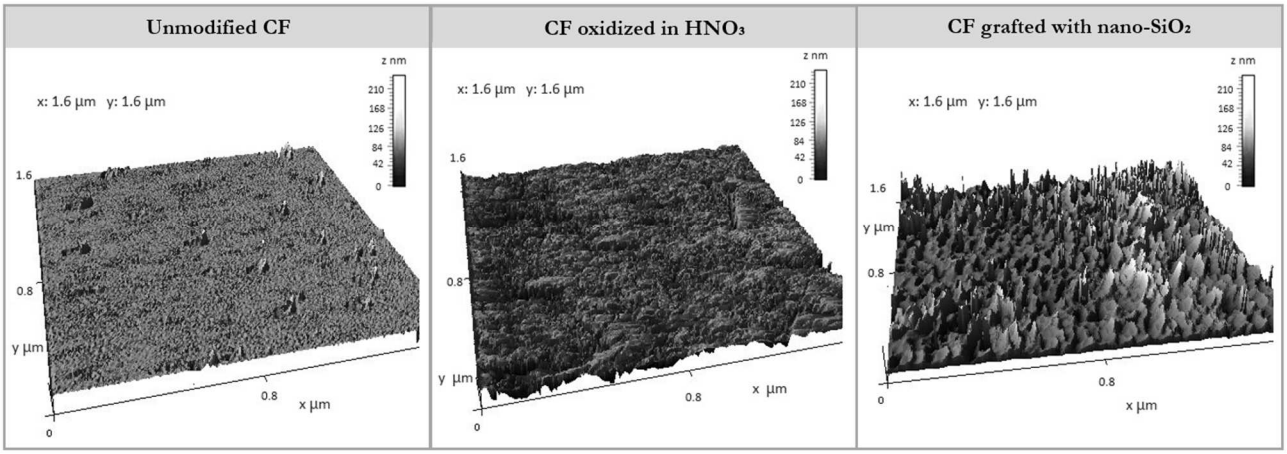


***Fig. 3*** *Surface topography of the carbon fibres*

***Tab. 3*** *Surface roughness parameters of short carbon fibres*

| Modification of short carbon fibres | Ra [nm] | Rq [nm] |
|---|---|---|
| Unmodified | 71 | 87 |
| Oxidized in $HNO_3$ | 85 | 104 |
| Grafted with nano-$SiO_2$ | 102 | 119 |

The AFM was also utilized to investigate the topography of the individual composites. Examples are illustrated in the Fig. 4. The distribution of CF bundles within the PA6 matrix varied depending on their concentration in the composite. Compared to the polymer without filler, the CF caused slight inhomogeneities. The composites featuring modified CF exhibited a more organized structure. The values of the surface roughness parameters Ra and Rq of the composites obtained by the AFM software are listed in the Tab. 4. The average roughness of the reference sample was Ra=0.56 μm and Rq = 0.61 μm. In general, the surface roughness of the PA6-CF composites increased with the percentage of the CF filler. The roughness values did not exhibit significant difference depending on the used CF treatment method. Besides the CF content, the surface roughness is also influenced by processing technology and selected processing parameters [32], [33].

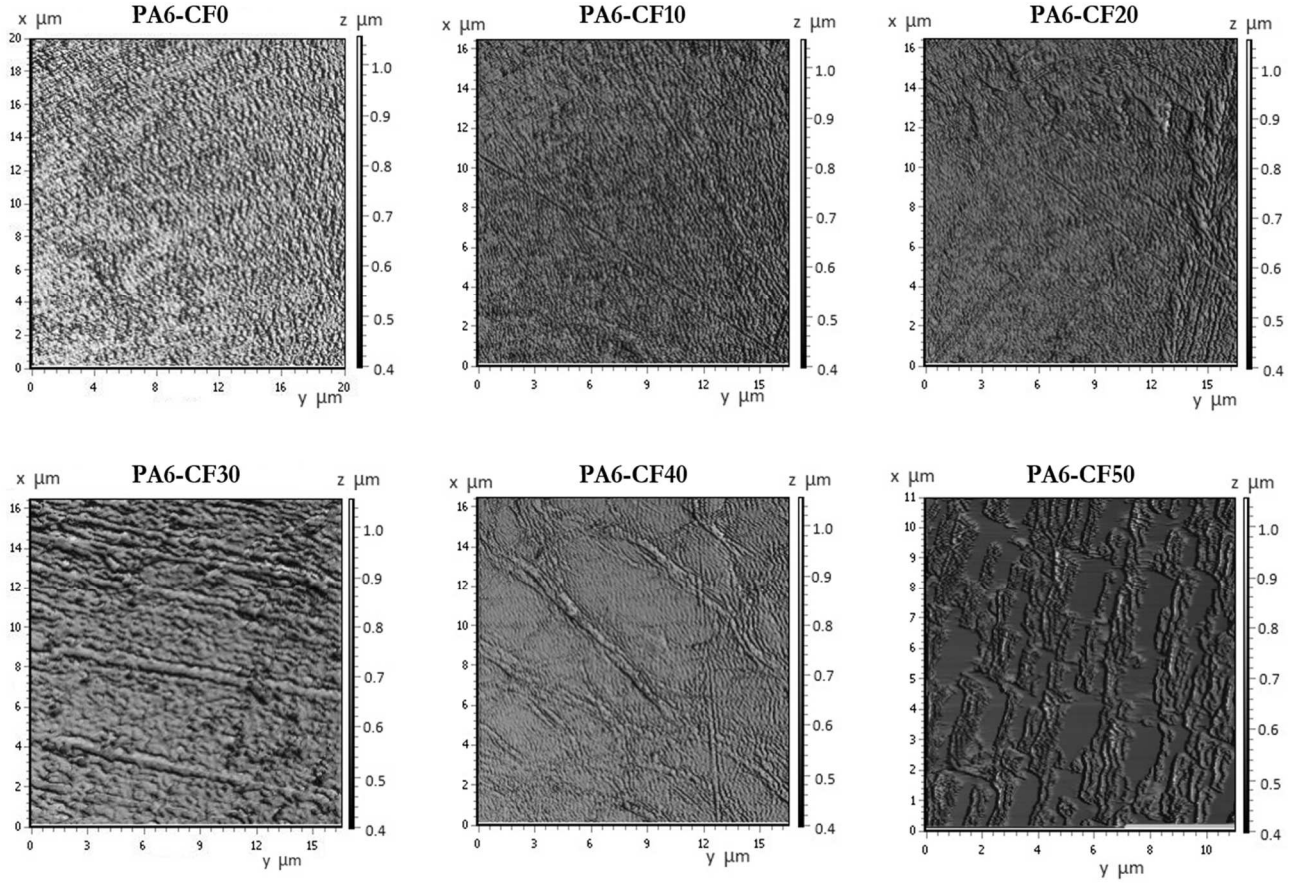


***Fig. 4*** *Topography examples of the PA6 and PA6 composites reinforced with the CF grafted with nano-$SiO_2$*

***Tab. 4*** *Roughness of PA6-CF composites*

| Sample and CF treatment | Ra [μm] | | | Rq [μm] | | |
|---|---|---|---|---|---|---|
| | unmodified | $HNO_3$ | Nano-$SiO_2$ | unmodified | $HNO_3$ | Nano-$SiO_2$ |
| **PA6-CF10** | 0.61 | 0.60 | 0.61 | 0.67 | 0.67 | 0.67 |
| **PA6-CF15** | 0.67 | 0.67 | 0.67 | 0.77 | 0.78 | 0.77 |
| **PA6-CF20** | 0.73 | 0.72 | 0.73 | 0.81 | 0.81 | 0.80 |
| **PA6-CF30** | 0.76 | 0.76 | 0.75 | 0.85 | 0.85 | 0.85 |
| **PA6-CF40** | 0.87 | 0.88 | 0.86 | 0.94 | 0.93 | 0.93 |
| **PA6-CF50** | 0.91 | 0.91 | 0.90 | 1.03 | 1.03 | 1.02 |
| **PA6-CF60** | 0.94 | 0.94 | 0.93 | 1.08 | 1.08 | 1.07 |

### 4.2 Mechanical properties

The tensile test results are shown in the Fig. 5. The addition of the CF to the polymer matrix significantly affects the tensile properties of the resulting composite, primarily due to the high strength and stiffness inherent in the CF. The tensile strength of the PA6-CF composites increased with the increasing filler content up to 40 wt%. The PA6-CF40 composites with the unmodified CF, the CF oxidized in $HNO_3$ and the CF grafted with nano-$SiO_2$ exhibited respective increases in tensile strength of 150.57%, 163.40%, and 176.57% compared to the reference sample PA6, with the tensile strength of 85.21 MPa. The addition of the CF grafted with nano-$SiO_2$ yielded the most substantial enhancement in tensile strength, reaching a peak of 235.78 MPa in the PA6-CF40 composite. However, beyond the CF content of 40 wt%, a decline in strength was observed. At high CF concentrations, filler agglomeration may arise, causing fibres to cluster into larger groups. This phenomenon compromises homogeneity, as even dispersion of filler within the polyamide matrix deteriorates, resulting in critical areas that may negatively affect overall strength. A similar trend was observed in the measured tensile modulus of PA-CF composites, that also exhibited a consistent rise with increasing filler content up to 40 wt% and then stagnated. The highest stiffness was achieved in PA6-CF40 composite with the CF grafted with nano-$SiO_2$, with the 779.06% increase in the tensile modulus (28.13 GPa) compared to the reference sample PA6 (3.20 GPa). With increasing stiffness of the composites, elongation at break decreased. The decline in elongation at break with the increasing CF content was observed up to 40 wt% and then plateaued. Compared to the reference sample (4.55%), the PA6-CF40 composite with CF grafted with nano-$SiO_2$ exhibited the most significant reduction of 62.41% in elongation at break, reaching 1.71%.

The flexural test results are shown in the Fig. 5. The flexural strength, similarly, to the tensile strength, increased with the increasing filler content up to 40 wt% and beyond this point, flexural strength decreased. The PA6-CF40 composite with nano-$SiO_2$ exhibited the highest flexural strength of 298.54 MPa, which is 165.79% increase compared to the PA6 (112.32 MPa). In the PA6-CF40 composites with the untreated CF, the flexural strength increased by 136.06%, and in the PA6-CF40 composites with the CF oxidized in $HNO_3$, it increased by 148.50% in comparison to the PA6.

The incorporation of the CF also improved the compressive properties of the resulting composites (Fig. 6). The compressive test results showed an increase in the compressive strength up to the CF content of 50 wt%. Additionally, the PA-CF composites grafted with nano-$SiO_2$ exhibited superior performance when compared to other CF variants. The compressive strength of unfilled PA6 was 110.23 MPa. An addition of 50 wt% of the unmodified CF, the CF oxidized in $HNO_3$ and the CF grafted with nano-$SiO_2$ resulted in a 128.1%, 135.73% and 144.53% increase of the compressive strength, respectively.

The Charpy tests were performed at temperatures of 20 °C and -30 °C. The results are shown in the Fig. 7. A significant increase in the Charpy notched impact strength with the increasing CF content was observed up to 40 wt%, followed by a plateau. The composite PA6-CF50 with the CF grafted with nano-$SiO_2$ exhibited the highest values of the Charpy notched impact strength, specifically 10.36 kJ/m² at 20 °C and 8.33 kJ/m² at -30 °C, which is a 106.37% and 109.82% increase in comparison to the reference PA6 sample. At a temperature of -30 °C, the Charpy notched impact strength of the tested materials was on average 15.88% lower than at a temperature of 20 °C. This is caused by a decrease in the mobility of polymer chains and their ability to deform and absorb energy during impacts at lower temperatures. The CF are characterized by high stiffness but lower ductility and in combination with a brittle polymer matrix due to sub-zero temperatures, it can contribute to brittle fracture behaviour and a decrease in the Charpy notched impact strength.

The Shore D hardness test results are depicted in the Fig. 7. The hardness increased, with an increasing CF content. The composite PA6-CF60 with CF grafted with nano-$SiO_2$ presented the highest hardness of 94.22 Shore D, which is 17.47% increase compared to PA6.

The test results indicate an improvement in mechanical properties attributable to the CF reinforcement. The PA6-CF composites showed an increase in stiffness, as mechanical load is transferred from the polyamide matrix to the CF. The high strength of the CF enables the composites to withstand higher loads without significant deformation or damage. This load transfer mechanism helps distribute the applied load more efficiently throughout the volume of the composite material, resulting in increased strength. A strong interaction between the matrix and the filler is essential to ensure effective load transfer. In the composites with the CF oxidized in $HNO_3$, the adhesion of the CF to the PA6 matrix improved, resulting in enhanced properties. Even better results were achieved when the CF, after oxidation in $HNO_3$, were grafted with nano-$SiO_2$. A significant improvement in properties was observed up to the content of 40 wt%. At higher concentrations of the CF, the agglomeration of the fibres can occur causing their inhomogeneous distribution in the PA6 matrix, which can negatively affect the resulting properties.

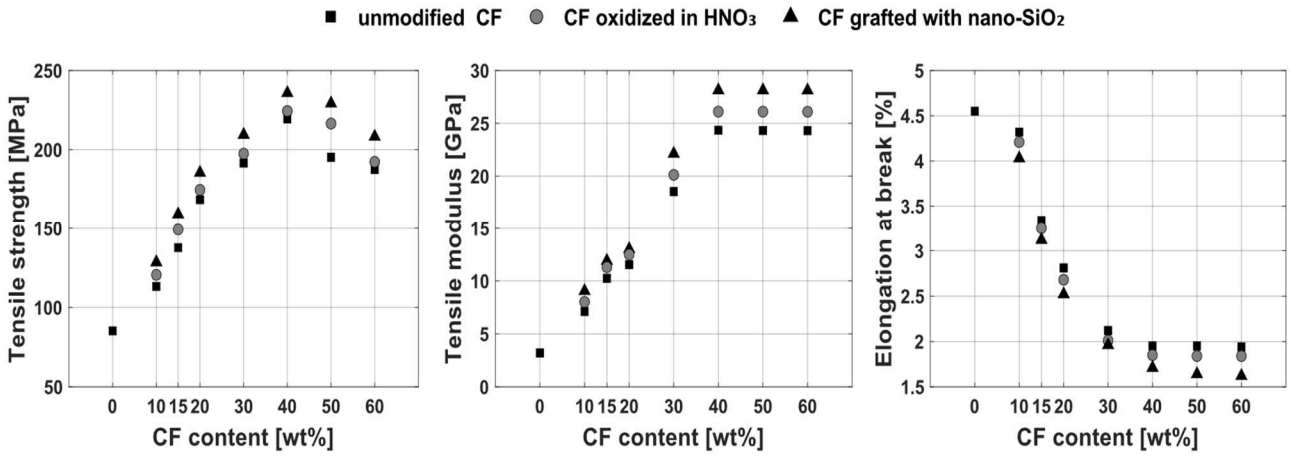


***Fig. 5*** *Tensile tests results*

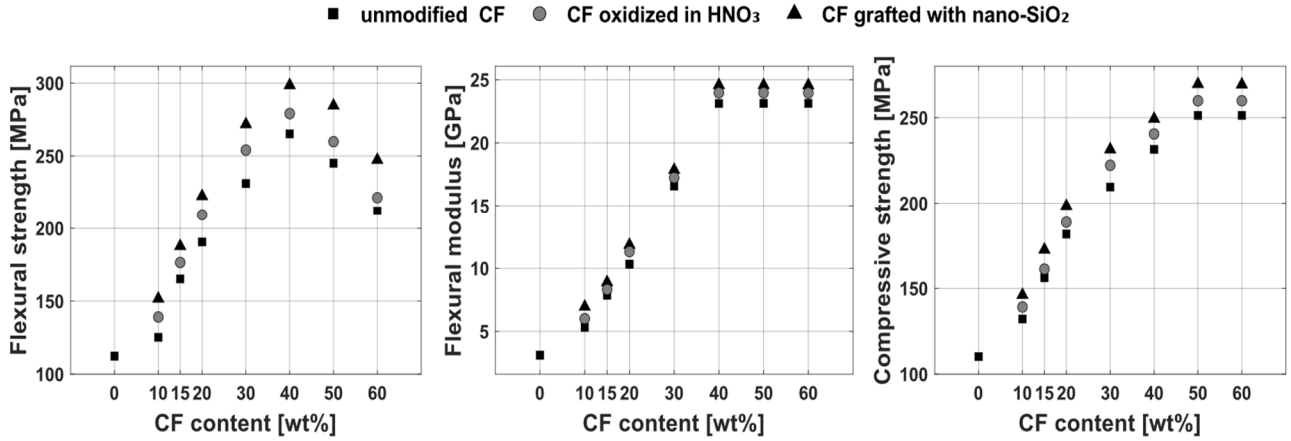


***Fig. 6*** *Flexural tests and compressive tests results*

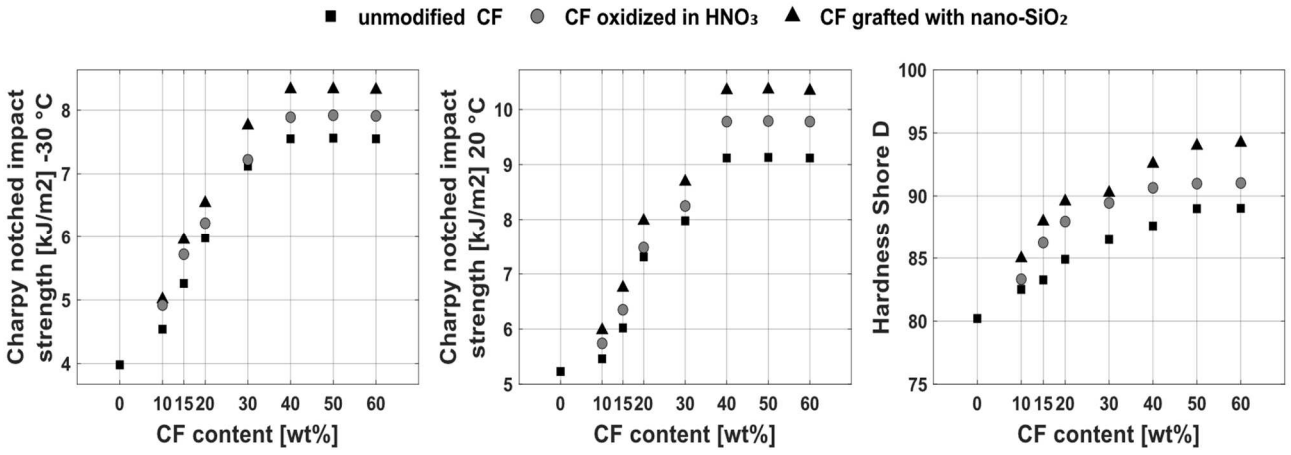


***Fig. 7*** *Charpy tests results and hardness tests results*

### 4.3 Dynamic mechanical analysis

The composites were subjected to DMA to obtain the temperature dependence and frequency dependence of the storage modulus $E'$, the loss modulus $E''$ and a tangent of the phase angle tan $\delta$. The selected results, including the reference PA6 sample and the composite materials PA6-CF with the CF contents of 10 wt% and 40 wt% are depicted in the Fig. 8 – 10.

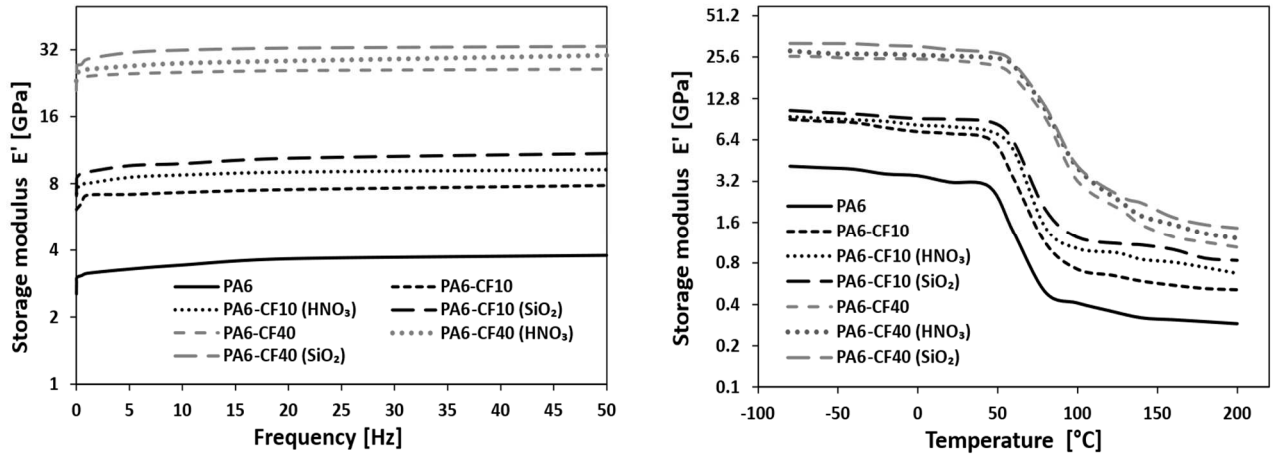


***Fig. 8*** *The DMA results – the storage modulus E': frequency sweep (0.1 – 50 Hz) at temperature 20 °C (left) and temperature sweep (-80 – 200 °C) at frequency 1 Hz (right)*

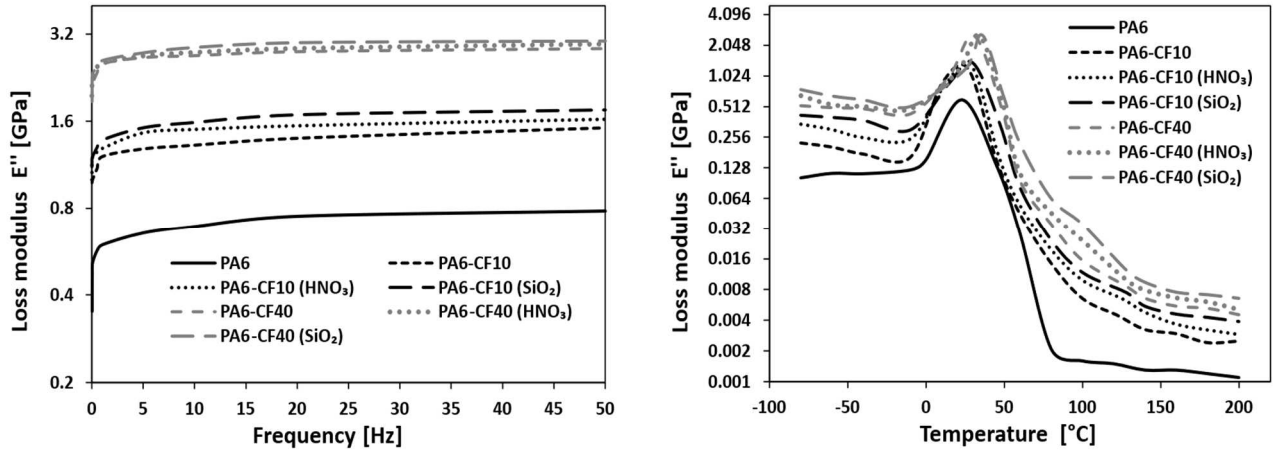


***Fig. 9*** *The DMA results – the storage modulus E'': frequency sweep (0.1 – 50 Hz) at temperature 20 °C (left) and temperature sweep (-80 – 200 °C) at frequency 1 Hz (right)*

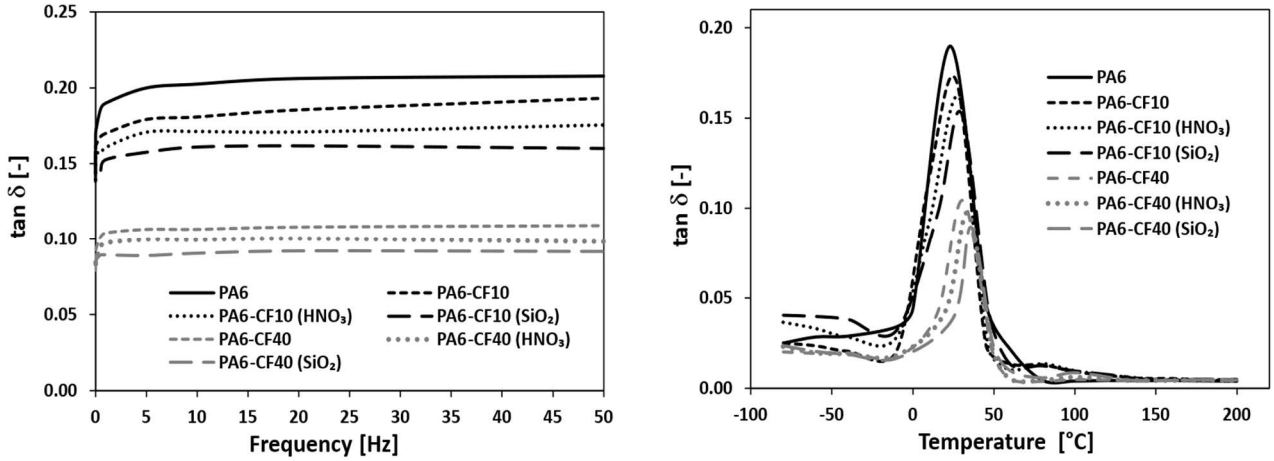


***Fig. 10*** *The DMA results – the tangent of phase angle tan δ: frequency sweep (0.1 – 50 Hz) at temperature 20 °C (left) and temperature sweep (-80 – 200 °C) at frequency 1 Hz (right)*

The storage modulus $E'$ of the tested composites increased with an increasing CF content up to 40 wt%, then it did not change significantly. The applied modifications of the CF increased the storage modulus. At low temperatures, the storage modulus exhibited relatively high values. This is because the movement of molecules in the polymer matrix slows down at lower temperatures, potentially leading to a change in crystalline structure, which significantly impacts the stiffness of the material. The mobility of polymer chains increases with temperature; consequently, the storage modulus decreases as the temperature rises. The values of the loss modulus $E''$ were significantly smaller than the values of the elastic modulus, which means that elastic properties prevail in the tested materials. Similarly to the $E'$, the loss modulus also exhibited notable increase with addition of the CF 40 wt%. Changes in a temperature dependence of the tangent of the phase angle tan $\delta$ indicate changes in material properties such as stiffness, damping, and energy dissipation. The width, height and position of the peaks reflect the nature and intensity of the relaxation processes occurring in the material. These relaxation processes may involve segmental motions of polymer chains, molecular rearrangements, or other viscoelastic phenomena. The peak of the tan $\delta$ decreased with the increasing CF content. The glass transition temperature $T_g$ of the reference PA6 material determined from the maximum temperature dependence of tan $\delta$ was around 45 °C. The addition of CF moved the $T_g$ slightly to higher temperatures, up to 49 °C. This shift was the most prominent in the samples with the larger content of the CF grafted with nano-$SiO_2$. Similar change of the $T_g$ in the PA-CF composites was also observed in the study [21]. The DMA frequency sweep findings indicate a slight rise in the elastic modulus (E'), loss modulus (E"), and tan $\delta$ across all materials as the frequency increases.

The incorporation of the CF into the polyamide matrix modifies the viscoelastic properties of the composite material by increasing stiffness, limiting the mobility of the polymer chain and reducing deformation, improving load transfer and also increasing resistance to elevated temperature. Proper surface treatments of the CF can improve adhesion to the matrix, thereby increasing the overall viscoelastic performance of the composite.

## 5 Conclusion

The incorporation of the carbon fibres into the polyamide matrix demonstrated a significant improvement in mechanical properties in all tested parameters. The reinforcing effect of the CF led to a significant improvement in the tensile, compressive and flexural strength. The stiffness and hardness of the resulting composites increased. This improvement can be attributed to the high strength and stiffness of the CF, which effectively reinforce the PA6 matrix. The DMA results showed that the incorporation of CF into the PA6 matrix has a significant effect on the dynamic-mechanical properties of the resulting composites. The presence of the CF contributed to an increase in storage modulus, an increase in dynamic stiffness and damping properties of the resulting composite materials. Furthermore, it can be inferred that the surface treatment of the CF, involving oxidation in $HNO_3$ followed be grafting with nano-$SiO_2$, significantly improved the mechanical properties of the resulting composite materials. This enhancement can be contributed to better adhesion between the CF and the PA6 matrix.

The resulting properties depend on many factors, such as filler dimensions, filler aspect ratio, uniformity of filler dispersion, and manufacturing processes. Further research may also focus on other factors such as temperature effects, environmental aging, and multiaxial loading to explore the potential of these composite materials in various engineering applications.

## Acknowledgement

***This research work was supported by the Operational Programme Integrated Infrastructure and cofinanced by the European Regional Development Fund through the Advancement and Support of Research and Development project for the "Centre for diagnostics and quality testing of materials" in the RIS3 SK specialization domain (acronym: CEDITEK II., ITMS2014+ code 313011W442. This research work was also created within the project „The use of the MATLAB program in the processing of experimental scientific data in materials research", code of project MVP01_2024, based on the financial support from the European Union within the call Early Stage Grants of the Recovery and Resilience Facility (Code of the project: 09I03-03-V05-00010, Component 9: More effective management and strengthening of research, development and innovation funding), and with the financial support of the Internal Grant Scheme of the Alexander Dubček University of Trenčín.***

## References

[1] MAŇAS, L., et al. (2019). Verification of material composition and manufacturing process of carbon fibre wheel. In: *Manufacturing Technology*, Vol. 19, No. 2, pp. 280-283. https://doi.org/10.21062/ujep/283.2019/a/1213-2489/MT/19/2/280.

[2] KUPČÁK, R., ZOUHAR, J. (2020). Application of composite materials in sports optics.

In: *Manufacturing Technology*, Vol. 20, No. 2, pp. 200-209. https://doi.org/10.21062/mft.2020.038.

[3] MAJKO, J., et al. (2022). Tensile properties of additively manufactured thermoplastic composites reinforced with chopped carbon fibre. In: *Materials*, Vol. 15, No, 12, pp. 4224. https://doi.org/10.3390/ma15124224.

[4] ALSHAMMARI, B.A., et al. (2021). Comprehensive review of the properties and modifications of carbon fiber-reinforced thermoplastic composites. In: *Polymers*, Vol. 13, No. 15, pp. 2474. https://doi.org/10.3390/polym13152474.

[5] ANSARI, M. S., ZAFAR, S., PATHAK, H. (2023). A comprehensive review of surface modification techniques for carbon fibers for enhanced performance of resulting composites. In: *Results in Surfaces and Interfaces*, Vol. 12: 100141. https://doi.org/10.1016/j.rsurfi.2023.100141.

[6] ZHENG, H., et al. (2022). Recent advances of interphases in carbon fiber-reinforced polymer composites: A review. In: *Composites Part B: Engineering*, Vol. 233, pp. 109639. https://doi.org/10.1016/j.compositesb.2022.109639.

[7] ZHAO, H., et al. (2023). Enhanced mechanical property of continuous carbon fiber/polyamide ther-moplastic composites by combinational treatments of carbon fiber fabric. In: *Composites Communications*, Vol. 38, pp. 101508. https://doi.org/10.1016/j.coco.2023.101508.

[8] IRISAWA, T., et al. (2018). The influence of oxygen containing functional groups on carbon fibers for mechanical properties and recyclability of CFRTPs made with in-situ polymerizable polyamide 6. In: *Composites Part A: Applied Science and Manufacturing*, Vol. 112, pp. 91-99. https://doi.org/10.1016/j.compositesa.2018.05.035.

[9] JIANG, J., et al. (2017). Influence of electrochemical oxidation of carbon fiber on the mechanical properties of carbon fiber/graphene oxide/epoxy composites. In: *Composites Part A: Applied Science and Manufacturing*, Vol. 95, pp. 248-256. https://doi.org/10.1016/j.compositesa.2017.02.004.

[10] ZHANG, T., et al. (2019). Interfacial adhesion between carbon fibers and nylon 6: Effect of fiber surface chemistry and grafting of nano-$SiO_2$. In: *Composites Part A: Applied Science and Manufacturing*, Vol. 121, pp. 157-168. https://doi.org/10.1016/j.compositesa.2019.03.029.

[11] AN, Q., et al. (2012). Electrophoretic deposition of carbon nanotubes onto carbon-fiber fabric for production of carbon/epoxy composites with improved mechanical properties. In: *Carbon*, Vol. 50, No. 11, pp. 4130-4143. https://doi.org/10.1016/j.carbon.2012.04.061.

[12] WU, Y., et al. (2020). Effect of electrophoretic deposition followed by solution pre-impregnated sur-face modified carbon fiber-carbon nanotubes on the mechanical properties of carbon fiber rein-forced polycarbonate composites. In: *Composites Part B: Engineering*, Vol. 195, pp. 108093. https://doi.org/10.1016/j.compositesb.2020.108093.

[13] KARSLI, N. G., et al. (2013). Effects of sizing materials on the properties of carbon fiber-reinforced polyamide 6,6 composites. In: *Polymer Composites*, Vol. 34, No. 10, pp. 1583-1590. https://doi.org/10.1002/pc.22556.

[14] CHO, B., et al. (2021) Interphase strengthening of carbon fiber/polyamide 6 composites through mixture of sizing agent and reduced graphene oxide coating. In: *Composites Part A: Applied Science and Manufacturing*, Vol. 149, pp. 106521. https://doi.org/10.1016/j.compositesa.2021.106521.

[15] KIM, B., et al. (2018). Synergistic interfacial reinforcement of carbon fiber/polyamide 6 composites us-ing carbon-nanotube-modified silane coating on ZnO-nanorod-grown carbon fiber. In: *Composites Sci-ence and Technology*, Vol. 16, pp. 362-372. https://doi.org/10.1016/j.compscitech.2018.07.015.

[16] YOU, J, et al. (2021) Carbon fiber-reinforced polyamide composites with efficient stress transfer via plasma-assisted mechanochemistry. In: *Composites Part C: Open Access*, Vol. 6, pp. 100209. https://doi.org/10.1016/j.jcomc.2021.100209.

[17] YUAN, J., et al. (2018) Surface modification of carbon fibers by microwave etching for epoxy resin composite. In: *Composites Science and Technology*, Vol. 164, pp. 222-228. https://doi.org/10.1016/j.compscitech.2018.05.043.

[18] FRANCISCO, D., et al (2019). Advances in polyamide nanocomposites: A review. In: *Polymer Composites*, 2019, Vol. 40, No. 3, pp. 851-870. https://doi.org/10.1002/pc.24837.

[19] MAJKO, J., et al. (2023). Challenges in Tensile Testing of Thermoplastic Composites Reinforced with Chopped Carbon Fibre Produced by Fused Filament Fabrication Method. In: *Manufacturing Technology*. Vol. 23, No. 2, pp. 216-224. https://doi.org/10.21062/mft.2023.010.

[20] QUAGLIATO, L., et al. (2020). The influence of fiber orientation and geometry-induced strain concentration on the fatigue life of short carbon fibers reinforced polyamide-6. In: *Materials & Design*, Vol. 190, pp. 108569. https://doi.org/10.1016/j.matdes.2020.108569.

[21] KARSLI, N. G., AYTAC, A. (2013). Tensile and thermomechanical properties of short carbon fiber reinforced polyamide 6 composites. In: *Composites Part B: Engineering*, Vol. 51, pp. 270-275. https://doi.org/10.1016/j.compositesb.2013.03.023.

[22] LIANG, J., et al. (2014). Mechanical properties, crystallization and melting behaviors of carbon fiber-reinforced PA6 composites. In: *Journal of Thermal Analysis and Calorimetry*, Vol. 115, pp: 209-218. https://doi.org/10.1007/s10973-013-3184-2.

[23] ARI, A., et al. (2023). Evaluation of the mechanical properties of chopped carbon fibre reinforced polypropylene, polyethylene, polyamide 6, and polyamide 12 composites. In: *Industria Textila*, Vol. 74, No. 2, pp. 175-183. https://doi.org/10.35530/it.074.02.202214.

[24] LIU, Y., et al. (2020). Effects of carbon nanotube length on interfacial properties of carbon fiber reinforced thermoplastic composites. In: *Journal of Materials Science*, Vol. 55, pp. 15467-15480. https://doi.org/10.1007/s10853-020-05129-w.

[25] LI, B., et al. (2023). Improving mechanical and thermal properties of short carbon fiber/polyamide 6 composites through a polydopamine/nano-silica interface layer. In: *Journal of Applied Polymer Science*, Vol. 140, No. 6, pp. e53457. https://doi.org/10.1002/app.53457.

[26] JING, X., et al. (2023). Polyurethane with nano-$SiO_2$ based surface sizing method for 3D printed carbon fiber reinforced nylon 6 composites. In: *Polymer Composites*, Vol. 44, No. 3, pp. 1546-1561. https://doi.org/10.1002/pc.27187.

[27] MA, Y., et al. (2018). Enhanced interfacial properties of carbon fiber reinforced polyamide 6 composites by grafting graphene oxide onto fiber surface. In: *Applied Surface Science*, Vol. 452, pp. 286-298. https://doi.org/10.1016/j.apsusc.2018.04.274.

[28] SINGH, R., et al. (2018). On the applicability of composite PA6-TiO2 filaments for the rapid prototyping of innovative materials and structures. In: *Composites Part B: Engineering*, Vol. 143, pp. 132-140. https://doi.org/10.1016/j.compositesb.2018.01.032.

[29] VOIGTLÄNDER, B. (2015). Scanning probe microscopy: Atomic force microscopy and scanning tunneling microscopy. Springer. ISBN 978-3-662-45240-0.

[30] BELLITTO, V. (2012). Atomic force microscopy: imaging, measuring and manipulating surfaces at the atomic scale. BoD–Books on Demand. ISBN 978-953-51-0414-8.

[31] LI, L., WU, D., HE, M. (2020). Electrophoretic Deposition of Chitosan-modified Carbon Fiber to Enhance Hygrothermal and Mechanical Properties of Carbon Fiber/Polyamide 6 Composites. In: *Fibers and Polymers*, Vol. 21, No. 3, pp. 583-589. https://doi.org/10.1007/s12221-020-9280-6.

[32] BIGERELLE, M., et al. (2008). Multiscale roughness analysis in injection-molding process. In: *Polymer Engineering & Science*, Vol. 48, No. 9, pp. 1725-1736. https://doi.org/10.1002/pen.21131.

[33] BOZDEMIR, M. (2018). Prediction of surface roughness considering cutting parameters and humidi-ty condition in end milling of polyamide materials. In: *Computational intelligence and neuroscience*, Vol .1, pp. 5850432. https://doi.org/10.1155/2018/5850432.